Journal Name

EDGE ARTICLE

Metabolic labelling of cholesteryl glucosides in *Helicobacter pylori* reveals how uptake of human lipids enhances bacterial virulence

Hau-Ming Jan,[a,b,‡] Yi-Chi Chen,[a,b,‡] Yu-Yin Shih,[a] Yu-Chen Huang,[c] Zhijay Tu,[a] Arun B. Ingle,[f] Sheng-Wen Liu,[a] Ming-Shiang Wu,[d] Jacquelyn Gervay-Hague,[e] Kwok-Kong Tony Mong,[f] Yet-Ran Chen[c] and Chun-Hung Lin[*,a,b]

Helicobacter pylori infects approximately half of the human population and is the main cause of various gastric diseases. This pathogen is auxotrophic for cholesterol, which it converts upon uptake to various cholesteryl α-glucoside derivatives, including cholesteryl 6′-acyl and 6′-phosphatidyl α-glucosides (CAGs and CPGs). Owing to a lack of sensitive analytical methods, it is not known if CAGs and CPGs play distinct physiological roles or how the acyl chain component affects function. Herein we established a metabolite-labelling method for characterizing these derivatives qualitatively and quantitatively with a femtomolar detection limit. The development generated an MS/MS database of CGds, allowing for profiling of all the cholesterol-derived metabolites. The subsequent analysis led to the unprecedented information that these bacteria acquire phospholipids from the membrane of epithelial cells for CAG biosynthesis. The resulting increase in longer or/and unsaturated CAG acyl chains helped to promote lipid raft formation and thus delivery of the virulence factor CagA into the host cell, supporting the idea that the host/pathogen interplay enhances bacterial virulence. These findings demonstrate an important connection between the chain length of CAGs and the bacterial pathogenicity.

Introduction

Infecting ~50% of the world population, *Helicobacter pylori* causes chronic gastritis, which is asymptomatic in the majority of carriers but is considered a major risk factor for development of gastric and duodenal ulcers and gastric malignancies, including mucosa-associated lymphoid tissue lymphoma and gastric adenocarcinoma.[1] This bacterium has an exceptional ability to persist and establish chronic infection, unlike other Gram-negative bacterial pathogens, and represents a highly successful pathogen because it is capable of evading, subverting and manipulating the host's immune system.[2, 3] For example, cytotoxin-associated gene A (CagA)[4] is an *H. pylori* virulence factor that enters host cells via type IV secretion system (T4SS)–mediated translocation.[5] CagA then undergoes tyrosine phosphorylation by c-Src family kinases,[6, 7]

and the phosphorylated CagA then activates several cellular signalling processes, including those leading to cancer development.[8, 9] Interestingly the translocation process is not restricted to transfer from *H. pylori* to the host. The pathogen also receives molecules such as L-fucose[10] and cholesterol[3, 11, 12] from the host for various purposes.

H. pylori assimilates cholesterol into its membrane by taking up cholesterol from the medium or from epithelial cells of the stomach.[13] Upon uptake, the bacterial cells modify the cholesterol by α-glucosylation. Specifically, the glucosyltransferase encoded by *hp0421* catalyses transfer of glucose to the 3β-hydroxyl group of cholesterol, yielding cholesteryl α-D-glucopyranoside (CG). An acyl or phosphatidyl group is then attached to O6′ of glucose in CG to produce cholesteryl-6′-*O*-acyl-α-D-glucopyranoside (CAG) or cholesteryl-6′-*O*-phosphatidyl-α-D-glucopyranoside (CPG), respectively.[14, 15] These cholesteryl glucoside derivatives (CGds) have been shown to be essential for several physiological activities, such as antibiotic resistance,[12] CagA translocation,[16] prevention of phagocytosis by macrophages,[3] and activation of invariant natural killer T cells.[17, 18] CAG and CPG are further diversified by addition of different fatty acid chains to the acyl and phosphatidyl groups, respectively. Owing to the limitation in purification and analysis, typically these CGds are examined collectively instead of being separated and compared to determine whether the acyl or phosphatidyl chain plays a role in an activity of interest.

Herein we developed a specific metabolite-tagging method to facilitate the purification and characterization of *H. pylori*

a. Institute of Biological Chemistry, Academia Sinica, No. 128 Academia Road Section 2, Nan-Kang, Taipei, 11529, Taiwan
b. Institute of Biochemical Sciences and Department of Chemistry, National Taiwan University, Taipei, 10617, Taiwan
c. Agriculture Biotechnology Research Center, Academia Sinica, Taipei, 11529, Taiwan
d. Division of Gastroenterology, Department of Internal Medicine, National Taiwan University Hospital, Taipei, 10002, Taiwan
e. Department of Chemistry, University of California, Davis, CA, 95618, USA
f. Department of Applied Chemistry, National Chiao-Tung University, Hsin-Chu 300, Taiwan
† Electronic supplementary information (ESI) available: General reagents and instruments of chemical synthesis, supplementary schemes, synthetic procedures, supplementary spectra data of selected compounds, supplementary methods, supplementary figures and supplementary tables. See DOI: 10.1039/x0xx00000x
‡: These authors equally contributed to this work.
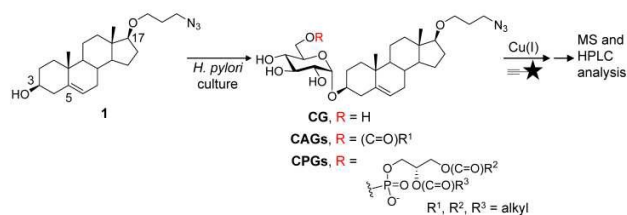
**Fig. 1** Schematic presentation of the metabolic labelling of *H. pylori* CGds. 17β-([3"-Azidopropoxy)-5-androsten-3β-ol (**1**; an azide-containing analogue of cholesterol) was added to *H. pylori* culture and incorporated into the biosynthetic pathway to produce various CGd analogues. After harvest and Folch extraction, these analogues were further reacted with a fluorescent alkyne (   ) via Cu(I)-catalysed 1,3-dipolar cycloaddition to give the conjugated products, which were then analysed by HPLC and MS.

CGds. Based on ultrahigh-performance liquid chromatography mass spectrometry (UPLC-MS), this method not only allowed structural determination and quantitative characterization of all CGds, but also offered a great advantage in detection sensitivity and isolation of various CGds that are difficultly obtained synthetically or by other means. Most importantly the resulting analysis demonstrated incorporation of host phospholipids led to a significant increase in CAGs containing longer or/and unsaturated fatty acid chains. This change was further found to promote translocation and subsequent phosphorylation of CagA through enhanced formation of lipid rafts, demonstrating an interactive strategy to enhance bacterial virulence.

Results

Synthesis and evaluation of tagged metabolites

Our metabolic labelling approach utilizes azide-containing cholesterol analogues in bacterial cell culture (Figure 1). After the cells were harvested, lipids were extracted and subjected to click chemistry (1,3-dipolar cycloaddition) with a fluorescently tagged alkyne. We first examined cholesterol analogues that are comparable with cholesterol in terms of biosynthetic incorporation *in vivo*. We synthesized three azide-containing cholesterol analogues, namely 17β-([3"-azidopropoxy)-5-androsten-3β-ol (compound **1**), 17β-([6"-azidohexanoxy)-5-androsten-3β-ol (**2**) and 17β-([9"-azidononanoxy)-5-androsten-3β-ol (**3**), as shown in supplementary scheme 1. These analogues all have the same four fused rings as cholesterol, but differ in the azide-containing side chain introduced at O17β. To evaluate if the three analogues are suitable for incorporation into the biosynthetic pathway, the cholesteryl α-glucosyltransferase gene *hp0421* was cloned and the protein overexpressed and purified as previously reported.[15] Steady-state kinetics analysis (Table S1)[19, 20] demonstrated that the catalytic efficiency (k_{cat}/K_m) values of compounds **1–3** are slightly smaller than that of cholesterol, in the range of 84–59% that of cholesterol. **1** appeared to be the best among the three and was thus selected for further investigations. Moreover, four other cholesterol analogues (their structures of which are shown in
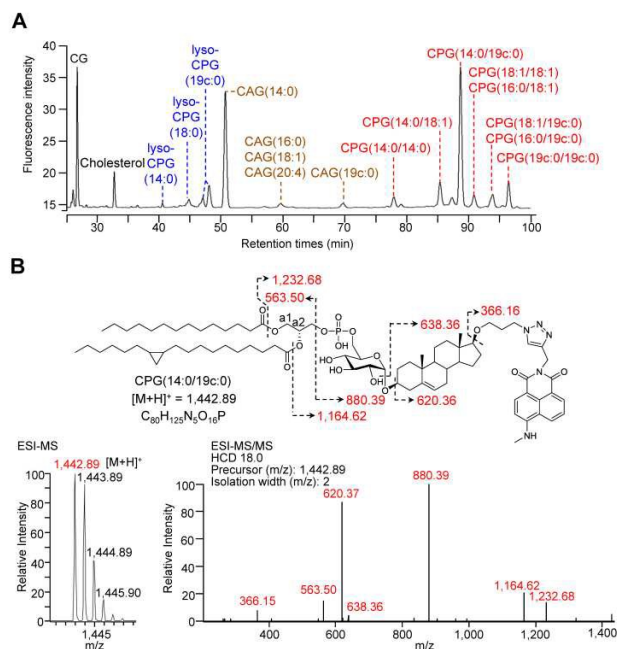
Fig. 2 HPLC separation and identification of various fluorophore-labelled CGds. (A) HPLC chromatogram of various labelled CGds including cholesterol, CG, CAGs, CPGs and lyso-CPGs. Compounds were detected by fluorescence (λ_{ex} = 428, λ_{em} = 528 nm). (B) Molecular structure and MS analysis of CPG(14:0/19c:0). The parent ion was identified by ESI-MS and the fragmented ions by ESI-MS/MS. The corresponding structures and molecular weights are indicated by dashed arrows and numbers.

Table S1) displayed much lower affinity for the enzyme, including ergosterol (13% that of cholesterol),[15] stigmasterol (7%),[15] 22-NBD-cholesterol (not detectable) and 25-NBD-cholesterol (not detectable; the last two compounds representing fluorescent analogues widely used for imaging studies[21-23]). The side chain at C17 appeared to be critical to the enzymatic glucosylation.

Compound **1** was evaluated by thin-layer chromatography and phospholipid composition analyses[24] to confirm that it is equivalent to cholesterol in the biosynthesis of CGds (Figure S1). The latter examined the levels of several phospholipids in addition to CPG. The results indicated that **1** and cholesterol yielded similar percentages of the major phospholipids in *H. pylori*, including phosphatidylethanolamine (PE), cardiolipin and phosphatidylglycerol.

We considered two factors when preparing suitable alkyne-containing fluorescent compounds for click chemistry, including reactivity (potential yield) and stability. Two fluorophore-possessing alkynes were designed and synthesized, such as 4-N-methylamino-1,8-napthalimidopropyne (MAN) and 4-*N,N*-dimethylamino-1,8-naphthalimidopropyne (DAN)[25] (supplementary scheme 2). Both MAN and DAN, as well as several commercially available fluorescent dyes (Figure S2B), were examined by Cu[I]-catalysed click chemistry. The reaction yield and stability of MAN were higher than those of DAN or other fluorescent dyes (Figure S2).

Structural determination and quantification of CGds

For the metabolic labelling of CGds, *H. pylori* was treated with **1** and grown under microaerobic conditions at 37 °C. After 4 days, the bacterial cells were collected and subjected to Folch extraction.[26] The extracts were reacted with MAN in the presence of tris(benzyltriazolylmethyl)amine, sodium ascorbate and $CuSO_4$ for 1 h. The resulting compounds were separated by high-performance liquid chromatography and detected by fluorescence (HPLC-fluorescence; C18-reversed-phase column; λ_{ex} = 428 nm, λ_{em} = 528 nm) (Figure 2A). The CGds were also identified by UPLC-MS in product ion scan mode. (Figure 2B, Figure S3 and Table S2).[27] HPLC-fluorescence analysis revealed fluorophore-conjugated analogues of cholesterol and CG plus three major groups of compounds, namely CAGs, CPGs and lyso-CPGs (these fluorophore-conjugated analogues of CAGs, CPGs and lyso-CPGs derived from **1** are hereafter referred to as CAGs, CPGs and lyso-CPGs, respectively, unless otherwise specified). These compounds appeared in three groups in the HPLC chromatogram due to differences in polarity. The structure of each compound was identified by MS and confirmed by tandem MS (MS/MS). The errors for the precursor m/z and for relative isotope abundance obtained by UPLC-MS were <5 ppm and 5%, respectively (Table S2). For instance, CPG(14:0/19c:0) (see Figure 2B for molecular structure) consists of two esterified fatty acids: myristic acid (14:0) and the other (19c:0) that contains a cyclopropane at C9 of the acyl chain.[28, 29] In the MS/MS analysis of CPG(14:0/19c:0), the predicted product ions for the functional groups of fatty acids, phosphate, glucose, steroid, triazole and 4-N-methylamino-1,8-napthalimide (the fluorophore) were observed (Figure 2B). The MS and corresponding MS/MS data for the other CGds are provided in Figure S3. We also performed ^1H, ^{13}C or/and ^{31}P NMR analysis of CPG(14:0/19c:0) and CAG(14:0) (supplementary spectra data 1, 2 and 3) to confirm that the phosphatidyl group is indeed attached to O6 of glucose and that C1 of the glucose forms an α-linkage with O3 of the steroid.[30] Phospholipases A1 and A2 (PLA1 and PLA2) were applied in UPLC-MS analysis[31, 32] to assign where the two fatty acid chains of CPG(14:0/19c:0) are attached to the phosphatidyl glycerol. The fatty acids (14:0) and (19c:0) were found to be specifically linked to a1- and a2-positions, respectively (Figure S4 A, B and C). It was noted that acyl migration occurred after cleavage of CPG(14:0/19c:0) at a1 using PLA1, i.e., the majority of the remaining ester at the a2 position moved to the a1 position via an intramolecular transfer (Figure S4 D, E and F).[33] Additionally, lyso-CPGs were found to exist as a mixture of regioisomers having the acyl chain attached to either the a1 or a2 position (Figure S4G). These are designated as 2-lyso-CPG(19c:0) or 1-lyso-CPG(19c:0), respectively, indicating that the ester at a2 or a1 is hydrolyzed.

HPLC-fluorescence and UPLC-MS/MS were employed to quantify the levels of CGds in *H. pylori*. The former was based on the integration of signals in the LC chromatogram, whereas the latter relied on the peak area of selected specific fragments for extracted ion chromatograms from the Orbitrap UPLC-MS operated in product ion scan mode. Table S3 shows
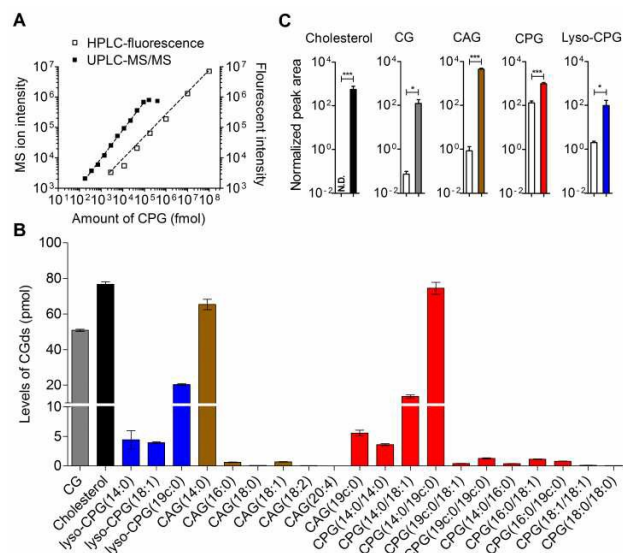
Fig. 3 Quantitative analysis of labelled CGds. (A) Calibration curves of CPG(14:0/19c:0) based on HPLC-fluorescence (λ_{ex} = 428, λ_{em} = 528 nm) and UPLC-MS/MS that was operated in the product ion scan mode with a specific fragment selected for extracted ion chromatography quantification. The dynamic ranges of UPLC-MS/MS and HPLC-fluorescence were 0.088–100 pmol and 2.8 pmol–100 nmol per 10^6 bacteria, respectively. (B) Levels of various CGds per 10^6 bacteria as analysed by UPLC-MS/MS. (C) Enhanced ionization efficiency of fluorophore-labeled CGds in the mass spectrometry. *H. pylori* cells were pre-treated with cholesterol (white bar) or compound **1** (gray bar) for two days. After harvest, the cholesterol-fed cells were extracted and directly analysed by UPLC-MS, whereas the **1**-pretreated cells were extracted, labeled with MAN by click reaction and then analysed by UPLC-MS. The normalized peak area was determined by the peak area of CGds divided by peak area of internal standard (phosphoinositol). N.D., Not Detected, denotes the ratio of signal to noise to be below three. Data shown were from three biological replicates. Error bars represent standard deviations. All statistically significant differences are indicated with asterisks; *P < 0.05, **P < 0.01, or ***P < 0.001 based on Student's t test.

the m/z of the designated target and fragmented ions, as well as the collision modes/energies. Chromatograms (Figure S5) shows the selected ion chromatograms of all CGds at m/z 366.16 or 620.36, which represent the m/z of fragmented ions (daughter ions) shown in Table S3. To quantify the CGds and determine the sensitivity of detection, CPG(14:0/19c:0) was purified to >99% purity (determined by HPLC-fluorescence and UPLC-MS) and used to establish calibration curves (Figure 3A) in a linear range between 2.8 pmol and 100 nmol per 10^6 bacteria for HPLC-fluorescence analysis, and between 0.088 and 100 pmol for UPLC-MS/MS. The calibration curves of CG, CAG(14:0), CPG(14:0/19c:0) and lyso-CPG(19c:0) using UPLC-MS/MS and HPLC-fluorescence are also shown in (Figure S6). In comparison with HPLC-fluorescence, UPLC-MS/MS was found to be more suitable for measuring CGds in very low abundance (<5 pmol per 10^6 bacteria), such as CAG(18:0), CAG(18:2), CPG(14:0/16:0) and CPG(18:0/18:0) (Figure 3B). The detection sensitivity in UPLC-MS/MS for the fluorophore-conjugated derivatives (0.088 pmol) was significantly enhanced relative to the unconjugated analogues, which is attributable to the dominant protonation of the incorporated fluorophore. In particular, whereas the native CG and CAGs
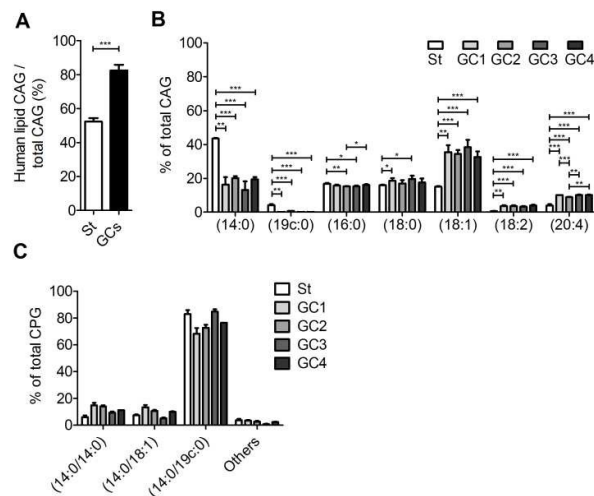
ARTICLE
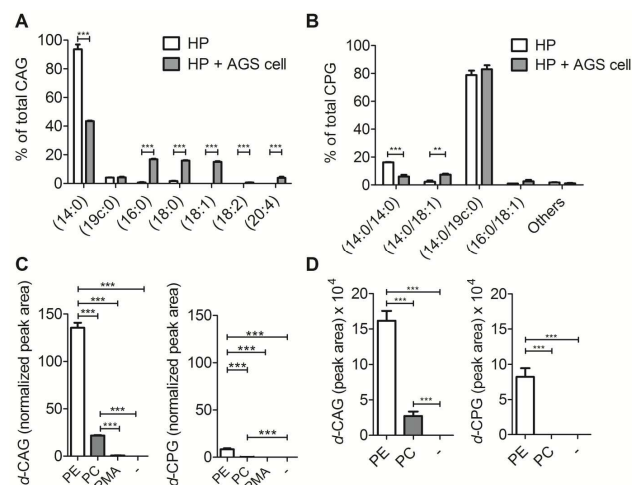
Fig. 4 Utilization of human lipids for CAG and CPG biosynthesis in *H. pylori*. Relative levels of (A) CAGs and (B) CPGs containing various acyl chains. *H. pylori* (HP; standard type, 26695) was incubated with or without human AGS cells for 6 h and then CAGs and CPGs were extracted from the cultures. "Others" includes the minor CPGs CPG(18:0/19c:0), CPG(19c:0/19c:0), CPG(18:0/18:0), CPG(16:0/18:1) and CPG(18:1/18:1). (C) Relative levels of deuterium-labelled CAG and CPG in the culture of *H. pylori*. *H. pylori* was treated with deuterium-labelled phosphatidylethanolamine (PE) or phosphatidylcholine (PC) or palmitic acid (PMA) for 7 h and then subjected to extensive washes to remove the unabsorbed compound. Both PE and PC contained deuterium-labelled palmitic acid (16:0) and unlabelled oleic acid (18:1). PMA contained deuterium-labelled palmitic acid (16:0). The levels of deuterium-labelled CAG and CPG (namely *d*-CAG and *d*-CPG, respectively) were quantified by UPLC-MS/MS and calculated based on the abundance of spiked internal standard (phosphoinositol). (D) Incorporation of deuterium-labelled fatty acids from phospholipids into CAGs and CPGs. AGS cells were treated with deuterium-labelled PE or PC for 1 h and then infected with *H. pylori* (26695) for 6 h. PE and PC contained deuterium-labelled palmitic acid (16:0) and unlabelled oleic acid (18:1). The levels of deuterium-labelled CAGs and CPGs (*d*-CAG and *d*-CPG, respectively) were determined by the area of the product ion signals in the UPLC-MS spectra. Data shown are from three biological replicates. Error bars represent standard deviations. All statistically significant differences are indicated with asterisks; **P < 0.01 or ***P < 0.001 based on Student's t test.

Fig. 5 Utilization of human lipids for CAG biosynthesis in standard type *H. pylori* and clinical strains from patients with gastric cancer. Standard type *H. pylori* (St; 26695) and clinical isolates (GC1–GC4) were cultured with AGS cells, and the amounts of CAGs containing different fatty acid chains were measured by UPLC-MS. (A) Ratio of human-lipid-containing CAGs to total CAGs. (B) Relative levels of CAGs containing different acyl chains. Human-lipid-containing CAGs are composed of CAG(16:0), CAG(18:0), CAG(18:1), CAG(18:2) and CAG(20:4). Total CAGs also include CAG(14:0) and CAG(19c:0), which are predominant in *H. pylori*. (C) Relative levels of CPGs that contain different fatty acid chains in *H. pylori* 26695 (St) and the clinical strains isolated from patients of gastric cancer (GC1-CG4). "Others" represents the total of minor CPGs, including CPG(18:0/19c:0), CPG(19c:0/19c:0), CPG(18:0/18:0), CPG(16:0/18:1) and CPG(18:1/18:1). Data shown are from three biological replicates. Error bars represent standard deviations. All statistically significant differences are indicated with asterisks; *P < 0.05, **P < 0.01, or ***P < 0.001 based on Student's t test.

have no charge, the fluorophore-conjugated analogues had 100- and 10,000-fold enhanced intensities, respectively (Figure 3C).

Uptake of human phospholipids for CAG biosynthesis in *H. pylori*

We next applied these labelling and analysis methods to compare the lipid composition of CAGs and CPGs between *H. pylori* cultured alone and co-cultures of *H. pylori* with AGS cells (a human gastric cancer cell line; i.e., *H. pylori*-infected AGS cells). Two major CAGs were observed in the bacterial cells cultured alone (Figure 4A), namely CAG(14:0) (93.7%) and CAG(19c:0) (4.0%), in agreement with the fact that these two fatty acids are dominant in *H. pylori*.[14] In contrast, the co-cultured *H. pylori* generated significant amounts of CAGs that contain longer or/and unsaturated acyl chains, such as CAG(16:0), CAG(18:0), CAG(18:1), CAG(18:2) and CAG(20:4) (Figure 4A and Figure S7A). These lipid chains rarely exist in *H. pylori* cultures, suggesting that they may have originated from the human cells. Contrary to prediction, there was no obvious

difference in the lipid compositions or percentages of CPGs between the bacterial culture and the co-culture (Figure 4B and Figure S7B).

We further examined the CAG and CPG compositions when AGS cells were co-cultured with different strains of *H. pylori*, including the standard type (26695) and four clinical strains isolated from patients with gastric cancer (GC1–GC4). UPLC-MS analysis indicated that on average 83% of the total CAGs obtained from the clinical isolates had incorporated human fatty acid chains, including (16:0), (18:0), (18:1), (18:2) and (20:4). In contrast, an average of 52% of CAGs from *H. pylori* 26695 showed such incorporation (Figure 5A). In particular, the GC1–GC4 strains contained a higher content of CAG(18:1), CAG(18:2) and CAG(20:4) (Figure 5B) which have one or more double bonds. There was no obvious difference in the lipid composition of CPGs among any of these *H. pylori* strains (Figure 5C).

To search for a possible precursor in the biosynthesis, we first treated *H. pylori* cultures with deuterium-labelled PE, phosphatidylcholine (PC) or palmitic acid (16:0) for 7 h to examine the incorporation of deuterium-labelled acyl chains in CAGs and CPGs. PE was found to be the major precursor in the biosynthesis of CAGs and CPGs, although PC was also incorporated into CAGs to a small extent (Figure 4C). Next, AGS cells were pretreated with **1** for 24 h, incubated with deuterium-labelled PE or PC (the two major phospholipids in
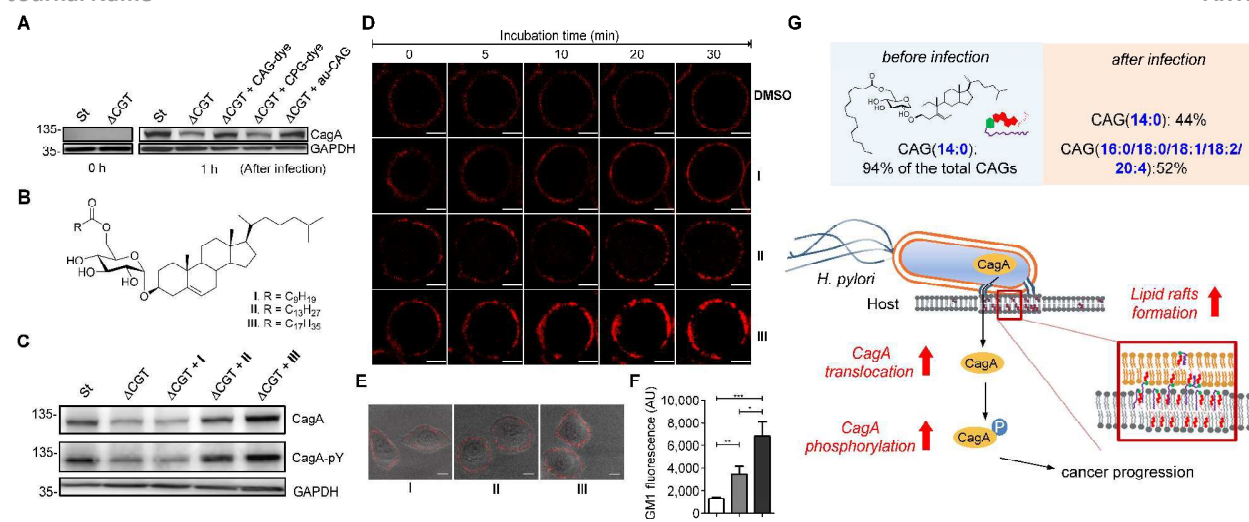
Fig. 6 Extent of CagA translocation and lipid rafts formation under various conditions. (A) CagA translocation in AGS cells cultured for 4 h with *H. pylori* 26695 (St), a cholesterol glucosyltransferase−deficient strain (ΔCGT), or ΔCGT pretreated for 30 min with fluorescently labelled CAG(14:0) (CAG-dye), fluorescently labelled CPG(14:0/19c:0) (CPG-dye), or authentic CAG(14:0) (au-CAG). Translocated CagA was detected by immunoblotting before and 1 h after infection. (B) Structures of CAGs containing an O6′ ester of decanoic acid (**I**), myristic acid (**II**) and stearic acid (**III**). **I** carries the shortest fatty acid chain; **II** and **III** carry the most abundant fatty acid chains in *H. pylori* and humans, respectively. (C) Effects of CAGs with different acyl chains on CagA translocation and CagA tyrosine phosphorylation as detected by immunoblotting after co-culture of AGS cells with *H. pylori* strains as described in (A). (D) Time-lapse images of AGS cells that were treated with CAGs (**I**, **II** or **III**). Lipid rafts (GM1) in AGS cells were first labelled with Alexa Fluor 594-conjugated cholera toxin subunit β, followed by the treatment with indicated CAGs (10:0, 14:0 or 18:0) at 37 °C. Time-lapse images were collected under a Zeiss LSM 510 confocal microscope at 0, 5, 10, 20 and 30 min. Scale bars, 5 μm. (E) Representative confocal immunofluorescence images for AGS cells that were first treated with CAGs (**I**, **II** or **III**) for 30 min prior to labelling of GM1. Scale bars, 10 μm. (F) Quantitation of the fluorescent intensities measured in (E). At least 40 GM1-positive AGS cells from each treatment were scored for the quantitative analysis using ImageJ software. Statistical significance was evaluated using Student's *t*-test (*$P < 0.05$, **$P < 0.01$, or ***$P < 0.001$). (G) The figure demonstrates how uptake of human lipids enhances bacterial virulence. The resulting uptake altered bacterial CAG compositions (especially CAGs containing longer or/and unsaturated fatty acid chains), leading to a higher level of CagA translocation and lipid raft formation.

human cells) for 1 h. Because it is important to rule out the possibility of adsorbing any lipids from culture dishes during *H. pylori* infection process, we extensively washed the phospholipid-pretreated AGS cells with phosphate-buffered saline (PBS) and then transferred the cells to new plates. The incorporation of each phospholipid into AGS cells was monitored by UPLC-MS. The cells were subsequently infected with *H. pylori* 26695 for 6 h and analysed by UPLC-MS to determine the proportion of deuterium-labelled CAGs and CPGs. The analysis supported the previous observation and demonstrated PE to be the primary source for the acyl chains of CAGs and CPGs (Figure 4D), and that the bacteria can obtain phospholipids from the host cell for synthesis of CAGs and CPGs. CPGs appeared to have a much lower level of incorporation of host phospholipids than CAGs (Figure S7 C and D).

Enhanced CagA translocation and lipid raft formation by CAGs containing longer acyl chains

Because we were able to isolate individual CAGs and CPGs, we further investigated the degree of influence of each derivative on physiological activities. In the study of CagA translocation, we compared *H. pylori* 26695 to ΔCGT (a cholesterol glucosyltransferase−deficient strain (was prepared as previously reported[16]) and to ΔCGT pretreated for 30 min with either authentic CAG(14:0) (synthesized as previously reported[34]), fluorophore-labelled CAG(14:0), or fluorophore-labelled CPG(14:0/19c:0) (Figure 6A). CAG(14:0) and CPG(14:0/19c:0) are the most abundant CAG and CPG in *H. pylori*, respectively. AGS cells were infected with the *H. pylori* strains for 1 h, and cell extracts were immunoblotted with a CagA-specific monoclonal antibody. There was no obvious difference between pretreatment with labelled and authentic CAG, indicating that fluorophore-conjugated CGd analogues are comparable to the corresponding native CGds and could be purified individually for further investigation. Additionally, CAG was found, for the first time, to promote a higher degree of CagA translocation than CPG (Figure 6B). The result with authentic CAG was similar to that of the positive control (*H. pylori* 26695), indicating that CAGs are likely responsible for the observed activity among the mixture of CGds.

We further investigated the effect of chain length on activity of CAGs. ΔCGT was pretreated for 30 min with three CAGs of increasing chain length (CAG(10:0), CAG(14:0) and CAG(18:0); Figure 6B) and used to infect AGS cells. Analysis of CagA translocation and the subsequent tyrosine phosphorylation[35] demonstrated that the acyl chain length of CAGs indeed plays a critical role in these activities (Figure 6C). The degree of CagA translocation and the corresponding phosphorylation increased with increasing chain length.

In addition, we examined whether the chain length of CAGs correlates with lipid raft formation. Time-lapse fluorescence microscopy was performed to monitor the mobilization of ganglioside GM1−associated rafts after each CAG was added

Chemical Science Accepted Manuscript

to AGS cells. GM1 in AGS cells was labelled with Alexa-594-cholera toxin prior to treatment with CAG(10:0), CAG(14:0) or CAG(18:0). We found a time-dependent increase in fluorescence intensity for all three CAGs, and further found that CAG(18:0) induced the greatest accumulation of GM1 (Figure 6D and Supplementary movies). Furthermore, when AGS cells were treated with CAG(10:0), CAG(14:0) or CAG(18:0) for 30 min and then labelled with GM1, the GM1 fluorescence intensity increased with increasing chain length (Figure 6E and 6F). Taken together, these results suggest that CAGs with incorporated human fatty acids enhance formation of lipid rafts in the membrane, which may lead to higher levels of CagA translocation and subsequent phosphorylation.

Discussion

Click chemistry-based tagging methods have been prevalently used in metabolite analysis. Our development appears to provide several advantages. Firstly, the introduced fluorophore MAN is readily protonated in solution, significantly enhancing the ionization level in mass spectrometry (10^2 to 10^5-fold depending on the type of CGds). The combined mass spectrometric detection and enhanced ionization of tagged metabolites made it possible to reach the detection limit at femtomolar level. Secondly, MAN was found to display much higher stability in comparison with several commercial fluorescent dyes (Figure S2B). The beneficial features of high sensitivity and stability support the idea that MAN should be useful to other profiling studies. Thirdly, conventional analysis (e.g. 2D thin layer chromatography) is usually entangled with the contamination of phospholipids, explaining the reason why the relevant isolation or purification becomes troublesome. In contrast, our development makes the entire process more robust and it takes 2-3 weeks to obtain a single cholestyl glucosde derivative at mg level, including 7-10 days of culturing bacteria. After harvest, any of CGds can be readily available with >95% purity after bacterial cells are subjected to extraction with organic solvents, followed by two steps of column chromatography. Furthermore, the use of azide-containing compound **1** and the fluorophore MAN is compatible for the purpose of fluorescent imaging to demonstrate how these labeled CGds are translocated to or/and distributed in host cell.

Previous findings on the uptake of L-fucose from the host by *H. pylori* indicate that this is a beneficial strategy to acquire additional carbon and energy, as well as to evade host immune surveillance.[10] Likewise, *H. pylori* has evolved to derive various CGds from exogenous cholesterol, for which it is auxotrophic (lacking the biosynthetic machinery) but which is indispensible for its pathogenesis and virulence.[3, 11, 14] In this study, by using a specific labelling method, we demonstrated that *H. pylori* also acquires phospholipids from the host for CAG biosynthesis. The acyl chain composition of *H. pylori* CAGs dramatically changed in the presence of human host cells. For instance, CAG(14:0) constituted 94% of the total CAGs when bacteria were cultured alone, whereas when bacteria were cultured with human cells, CAG(14:0) was reduced to 44% and

was accompanied by CAGs containing human fatty acid chains (52%; (16:0), (18:0), (18:1), (18:2) and (20:4); Figure 4A and Figure S7A). This alteration led to a higher level of CagA translocation, indicating that accessing human phospholipids enhances bacterial virulence by altering bacterial CAG compositions (Figure 6G). Interestingly, Hatakeyama *et al.* found that host phosphatidylserine is aberrantly externalized from the inner to the outer leaflet of the host plasma membrane at the site of *H. pylori* attachment, which facilitates the delivery, intracellular localization and pathophysiological activity of CagA.[36] This finding suggests a mechanism for the release of host phospholipids during bacterial infection.[36]

Cholesterol is an important component of cell membranes. Particularly in lipid rafts, this molecule serves as a glue to maintain close packing of lipids and proteins. *H. pylori* CGds can be considered modified versions of cholesterol with the additional attachment of glucose, acyl or/and phosphatidyl groups. CAGs, CPGs and lyso-CPGs likely have different roles in membranes. Wang *et al.* reported that CagA translocation is mediated in a cholesterol-dependent manner, as the formation of CGds from host cholesterol promotes the translocation of CagA by affecting membrane dynamics and enhancing lipid raft formation.[11, 16] Our study identified CAGs, but not CPGs, as being responsible for the enhanced translocation of CagA and formation of lipid rafts. Altered CAG composition therefore has multifaceted effects. Lipid rafts have been demonstrated to serve as the obligate structure for entry of bacterial and viral pathogens.[37, 38]

Our findings further demonstrated that only CAGs with longer acyl chains exert this effect to promote lipid raft formation and thus CagA translocation. This result is consistent with a number of previous reports. For instance, lipid rafts containing palmitoylated or stearoylated (C16/C18) GPI-anchored variant surface glycoprotein display a higher resistance to Triton X-100 extraction than those containing myristoylated (C14) GPI-anchored variant surface glycoprotein.[39, 40] Several raft-associated proteins are palmitoylated.[41, 42] When cytoplasmic proteins are subjected to lipidation, the presence of at least one palmitate chain, rather than the shorter myristoylate, is required for raft association.[40, 43] These studies support the idea that acquired host CAG(16:0) and CAG(18:0), rather than the plentiful bacterial CAG(14:0), assists in the formation of lipid rafts to enhance the subsequent CagA translocation.

We also demonstrated that bacterial strains obtained from patients with gastric cancer displayed a significant increase in CAGs carrying unsaturated acyl chains, i.e., CAG(18:1), CAG(18:2) and CAG(20:4). Brewster and Safran demonstrated that hybrid lipids (comprised of one fully saturated and one partially unsaturated chain) serve as a surface-active component by occupying the interface between the lipid raft (facing the saturated anchor) and the less ordered environment (facing the unsaturated chain).[44] These reports suggest that the unsaturated chains of CAG(18:1), CAG(18:2) and CAG(20:4) may contribute to raft structure by interacting with less-ordered lipids.

Steryl glycosides (SGs) are known to prevalently exist in many organisms and some of SGs are also acylated at C6' of the sugar moiety, like CAGs in *H. pylori*. In general, there are two possible routes regarding enzymatic acyl transfer; one requires acyl-CoA as the donor while the other one needs a different substrate for the same purpose. The acylation of several plant steryl glucosides were found to be independent of acyl-CoA. Instead, phosphoglycerolipids or/and galactolipids (fatty acids attached to C1 and C2) were employed for the enzymatic transfer of fatty acids.[45] In AGS cells, PE and PC are the major phospholipids. PE is also the major phospholipid in *H. pylori*. To search for a possible precursor in the biosynthesis of CAG, PE, PC and fatty acid (PMA) were individually added to the bacterial culture to examine the incorporation of exogenous acyl chains (i.e. deuterium-labeled acyl chains in CAG). As shown in Figure 4C, PE was found to be the major precursor in the biosynthesis of CAG. Little or no PMA was incorporated into CAGs. The result was in support of a lipid-dependent acyltransferase to be involved in the biosynthesis of CAGs, and PE to be a better substrate for this enzyme.

To explain the observed uptake of human phospholipids, it appears to be essential for understanding where the discussed acyltransferase is located in *H. pylori*, since the incorporation of deuterium-labelled acyl chain primarily occurred in CAGs but not in CPGs. We propose the CAG-related enzyme to reside at the bacterial outer membrane, making it possible for direct access of human phospholipids. As a matter of fact, several studies suggested that the biosynthetic location of CAGs is indispensible for their release to the surface of host cell and for the subsequent induction of the cytokines TNF-α and INF-γ.[18] On the other hand, the unknown phosphatidyltransferase, to convert CG to CPG, might be located at either the inner membrane or the cytoplasm, which hampers the access of host phospholipids.

Conclusions

We established a metabolite tagging method for robust detection of CGds at femtomolar sensitivity. The quantitative analysis of CGds indicated that these bacteria utilize phospholipids from human host cells to produce cholesteryl 6'-acyl α-glucosides (CAGs) that contain longer/unsaturated fatty acid chains. Our findings demonstrate, for the first time to our knowledge, the phospholipid hijack to be the key to augment the pathogenicity. Because the incorporated fluorophore displayed great inherent stability and high ionization degree in mass spectrometry, the development should be applicable to other metabolic profiling.

Experimental

Metabolic labelling of CGds

H. pylori cells were seeded on Brucella agar plates containing **1** (50 μM) for 2–4 days. Bacterial lipids were extracted by the Folch method,[26] redissolved in chloroform/methanol/water (5:4:1, v/v/v) and subjected to a click reaction with 0.25 mM MAN in the

presence of 1.25 mM TBTA, 12.5 mM sodium ascorbate, and 0.25 mM CuSO$_4$ at room temperature for 1 h. The solvent was removed *in vacuo*, and the dried residue was redissolved in chloroform/methanol/water (5:4:1, v/v/v) and analysed by HPLC and UPLC-MS.

HPLC analysis

For the experiments described in Figure 2A, an analytical Inspire C18 column (5 μm, 4.6 × 250 mm) was used at a flow rate of 0.4 mL/min. To obtain fluorophore-labelled CAG(14:0) and CPG(14:0/19c:0) for NMR characterization, a preparative Inspire C18 column (5 μm, 21.5 × 250 mm) was used at a flow rate of 6.5 mL/min. For quantification of CGds using HPLC-fluorescence, an analytical Inspire C18 column (5 μm, 4.6 × 250 mm) was used at a flow rate of 0.4 mL/min. In all experiments, eluent A contained 30% acetonitrile, 70% aqueous 20 mM ammonium acetate, and eluent B contained 90% isopropyl alcohol, 10% aqueous 20 mM ammonium acetate.

UPLC-MS analysis

UPLC-MS analysis was performed on a linear ion trap-Orbitrap mass spectrometer (Orbitrap Elite; Thermo Fisher Scientific) coupled online with a UPLC system (ACQUITY UPLC; Waters). The mass spectrometer was operated in the positive electrospray ion mode set to one full FT-MS scan (m/z 200−1,600; 15,000 resolution) and switched to different FT-MS product ion scans (15,000 resolution) for the different CGd precursors. CGds were separated on a CSH C18 column (1.7 μm, 100 x 2.1 mm; Waters, USA) using gradients of LC buffer A (10 mM ammonium acetate in 40:60 [v/v] acetonitrile/water) and LC buffer B (10 mM ammonium acetate in 90:10 [v/v] isopropyl alcohol/acetonitrile) at a flow rate of 0.4 mL/min. To normalize the variations in sample preparation and UPLC-MS analysis, phosphatidylinositol containing deuterium-labelled palmitic acid (16:0) and unlabelled oleic acid (18:1) was used as the internal standard and added to the bacterial lysate (10^6 bacteria, determined by optical density at 600 nm). To determine the ionization efficiency of CGds with or without MAN labelling, the normalized peak area was defined as the peak area of CGds divided by the peak area of the internal standard. To quantify MAN-labelled CGds from bacterial lysates, the peak area of selected specific fragments for extracted ion chromatograms was used. To establish the calibration curves of CGds, we added purified MAN-labelled cholesterol, CG, CAG(14:0), CPG(14:0/19c:0) and Lyso-CPG(19c:0) to the lysate from 10^6 bacteria along with the click chemistry reactants (TBTA, sodium ascorbate and CuSO$_4$). The calibration curves for quantitation were obtained by analyzing the peak areas of serially diluted standard (0.088, 0.176, 0.35, 0.7, 1.4, 2.8, 5.6, 11.25, 22.5, 45 and 90 pmol per 10^6 bacteria) measured by UPLC-MS operated in product ion scan mode. The amount of CGds in bacterial lysate was determined by comparing the peak area in lysate to standard curves. Relative isotopic abundance error was calculated as previously described.[27]

Co-culture experiments

Co-culture experiments were performed as previously described.[16] In the experiments described in Figures 4A, 4B and 5, AGS cells (8.0 × 10^6) were seeded in a 10-cm tissue culture dish and treated with **1**

(6.2 µg/mL) in Dulbecco's Modified Eagle Medium (DMEM) (Gibco, Invitrogen) at 37 °C for 16 h. AGS cells were infected with *H. pylori* (26695 or clinically isolated strains) at an MOI of 200:1 for 6 h and subsequently collected by centrifugation (6,000 × *g*) for 5 min. CGds-containing lipids were isolated by Folch extraction and fluorescently labelled by click reaction for UPLC-MS analysis. With respect to the study shown in Figure 4D, AGS cells (8.0×10^6) were seeded in a 10-cm tissue culture dish and treated with **1** (6.2 µg/mL) in DMEM at 37 °C for 16 h. To label AGS cells with deuterium-labelled phospholipid, AGS cells were incubated with serum-free medium (Ham's F12, Invitrogen) containing 0.1 mM 1-palmitoyl(d31)-2-oleoyl-*sn*-glycero-3-   phosphoethanolamine (dPOPE; 16:0 d31:(18:1)) or 0.1 mM 1-palmitoyl(d31)- 2-oleoyl-*sn*-glycero-3-phosphocholine (dPOPC; 16:0 d31:(18:1)) (Avanti Polar Lipids, USA) at 37 °C for 1 h. It is important to wash the cells with PBS five times to remove unbound **1** and dPOPE or dPOPC, and then transferred to a new plate for another 12 h. To demonstrate that bacterial uptake of deuterium-labelled phospholipids was from cells rather than phospholipids remaining on the culture dish, empty culture dishes were first treated **1** for 16 h, treated with POPE or dPOPC for another 1 h, washed with PBS five times, and then used to culture *H. pylori* without AGS cells for 6 h. No deuterium-labelled CGds were produced by *H. pylori* under these conditions. To perform infection experiments, unloaded or dPOPE/dPOPC-loaded AGS cells were infected with *H. pylori* (26695) at an MOI of 200:1 for 6 h and subsequently collected by centrifugation (6,000 × *g*) for 5 min. CGds-containing lipids were isolated by Folch extraction and fluorescently labelled by click reaction for UPLC-MS analysis. For CagA translocation experiments, AGS cells (8.0×10^5) were seeded in DMEM (Gibco, Invitrogen) in a 6-well culture plate at 37 °C for 16 h. To load *H. pylori* cells with CGds, *H. pylori* cells (26695 or ΔCGT) were incubated with serum-free medium (Ham's F12) containing 30 µM of MAN-labelled CAG(14:0), MAN-labelled CPG(14:0/19c:0), or unlabelled CAG standard at 37 °C for 30 min. The bacterial cells were then washed with PBS to remove unbound CPG or CAG and used to infect AGS cells at an MOI of 200:1 for 1 h.

Immunoprecipitation and blotting

After infection of AGS cells with *H. pylori* (MOI of ~200:1), cells were washed three times with PBS and collected with a cell scraper. To detect the internalized CagA to AGS cells, saponin was used to lyse AGS cells, but keep the bacteria intact.[5, 35] The AGS cells were gently lysed with PBS containing 0.1% saponin, protease inhibitor cocktail (Calbiochem, USA) and phosphatase inhibitor cocktail (Calbiochem, USA) for 10 min at room temperature. The cell debris and intact bacteria were separated from the soluble fraction by centrifugation (6,000 x *g* for 5 min), and the solute was filtered with a 0.22-µm-pore filter to obtain human cell proteins and the internalized CagA. The saponin lysis procedure was also performed on standard type *H. pylori* (26695) alone. Subsequent immunoprecipitation and blotting of CagA indicated that no CagA was detected, supporting the idea that this procedure did not release cytoplasmic proteins from *H. pylori* (data not shown). The filtrate (100 µg) was immunoprecipitated using 10 µg rabbit anti-CagA polyclonal antibody (Austral Biologicals, USA) and 30 µl Protein A Plus Agarose

(Thermo scientific, USA) at 4 °C overnight. The obtained precipitates were washed three times with immunoprecipitation buffer (25 mM Tris-HCl (pH 7.4), 150 mM NaCl, 5 mM EDTA, 1% Triton X-100) and once with TBS buffer (50 mM Tris-HCl, pH 7.4, 150 mM NaCl, 1 mM CaCl_2), then boiled in PAGE sample buffer (62.5 mM Tris-HCl, pH 6.8, 2% SDS, 10% (v/v) glycerol, 0.05% brilliant blue R) at 95 °C for 10 min, resolved by 6% SDS-PAGE, and transferred onto polyvinylidene difluoride membranes (Millipore, USA). The membranes were blocked with 5% (w/v) skim milk in TBS buffer containing 0.01% Tween 20 at room temperature for 1 h and incubated overnight with mouse monoclonal anti-CagA (Austral Biologicals; 1:2,000), mouse monoclonal anti-phosphotyrosine (4G10, Millipore; 1:2,000) or mouse monoclonal anti-GAPDH (ab9482, Abcam, UK; 1:5,000) at 4 °C. The blots were washed and incubated with HRP-conjugated secondary antibodies (Santa Cruz Biotechnology, USA) at a 1:5,000 dilution, and the proteins of interest were visualized using an enhanced chemiluminescence assay (WBKLS0500, Millipore). See supplementary methods for additional information.

Acknowledgements

Notes and references

1.   R. M. Peek, Jr. and M. J. Blaser, *Nat. Rev. Cancer*, 2002, **2**, 28-37.

2.   W. Khamri, A. P. Moran, M. L. Worku, Q. N. Karim, M. M. Walker, H. Annuk, J. A. Ferris, B. J. Appelmelk, P. Eggleton, K. B. Reid and M. R. Thursz, *Infect. Immun.*, 2005, **73**, 7677-7686.

3.   C. Wunder, Y. Churin, F. Winau, D. Warnecke, M. Vieth, B. Lindner, U. Zahringer, H. J. Mollenkopf, E. Heinz and T. F. Meyer, *Nat. Med.*, 2006, **12**, 1030-1038.

4.   S. Censini, C. Lange, Z. Xiang, J. E. Crabtree, P. Ghiara, M. Borodovsky, R. Rappuoli and A. Covacci, *Proc. Natl. Acad. Sci. U. S. A.*, 1996, **93**, 14648-14653.

5.   S. Odenbreit, J. Puls, B. Sedlmaier, E. Gerland, W. Fischer and R. Haas, *Science*, 2000, **287**, 1497-1500.

6.   H. Higashi, K. Yokoyama, Y. Fujii, S. Ren, H. Yuasa, I. Saadat, N. Murata-Kamiya, T. Azuma and M. Hatakeyama, *J. Biol. Chem.*, 2005, **280**, 23130-23137.

7.   M. Selbach, S. Moese, C. R. Hauck, T. F. Meyer and S. Backert, *J. Biol. Chem.*, 2002, **277**, 6775-6778.

8. H. Mimuro, T. Suzuki, S. Nagai, G. Rieder, M. Suzuki, T. Nagai, Y. Fujita, K. Nagamatsu, N. Ishijima, S. Koyasu, R. Haas and C. Sasakawa, *Cell Host Microbe*, 2007, **2**, 250-263.
9. L. Buti, E. Spooner, A. G. Van der Veen, R. Rappuoli, A. Covacci and H. L. Ploegh, *Proc. Natl. Acad. Sci. U. S. A.*, 2011, **108**, 9238-9243.
10. T. W. Liu, C. W. Ho, H. H. Huang, S. M. Chang, S. D. Popat, Y. T. Wang, M. S. Wu, Y. J. Chen and C. H. Lin, *Proc. Natl. Acad. Sci. U. S. A.*, 2009, **106**, 14581-14586.
11. C. H. Lai, Y. C. Chang, S. Y. Du, H. J. Wang, C. H. Kuo, S. H. Fang, H. W. Fu, H. H. Lin, A. S. Chiang and W. C. Wang, *Infect. immun.*, 2008, **76**, 3293-3303.
12. D. J. McGee, A. E. George, E. A. Trainor, K. E. Horton, E. Hildebrandt and T. L. Testerman, *Antimicrob. Agents Chemother.*, 2011, **55**, 2897-2904.
13. R. Ansorg, K. D. Muller, G. von Recklinghausen and H. P. Nalik, *Zentralblatt fur Bakteriologie : Int. J. Med. Microbiol.*, 1992, **276**, 323-329.
14. Y. Hirai, M. Haque, T. Yoshida, K. Yokota, T. Yasuda and K. Oguma, *J. bacteriol.*, 1995, **177**, 5327-5333.
15. A. H. Lebrun, C. Wunder, J. Hildebrand, Y. Churin, U. Zahringer, B. Lindner, T. F. Meyer, E. Heinz and D. Warnecke, *J. Biol. Chem.*, 2006, **281**, 27765-27772.
16. H. J. Wang, W. C. Cheng, H. H. Cheng, C. H. Lai and W. C. Wang, *Mol. Microbiol.*, 2012, **83**, 67-84.
17. Y. Ito, J. L. Vela, F. Matsumura, H. Hoshino, A. Tyznik, H. Lee, E. Girardi, D. M. Zajonc, R. Liddington, M. Kobayashi, X. Bao, J. Bugaytsova, T. Boren, R. Jin, Y. Zong, P. H. Seeberger, J. Nakayama, M. Kronenberg and M. Fukuda, *PLoS One*, 2013, **8**, e78191.
18. M. Shimamura, *Arch. Immunol. ther. Exp.*, 2012, **60**, 351-359.
19. P. Gonzalo, B. Sontag, D. Guillot and J. P. Reboud, *Anal. Biochem.*, 1995, **225**, 178-180.
20. H. Lee, P. Wang, H. Hoshino, Y. Ito, M. Kobayashi, J. Nakayama, P. H. Seeberger and M. Fukuda, *Glycobiology*, 2008, **18**, 549-558.
21. S. Mukherjee, X. Zha, I. Tabas and F. R. Maxfield, *Biophys. J.*, 1998, **75**, 1915-1925.
22. J. P. Slotte, *Biochim. Biophys. Acta.*, 1995, **1237**, 127-134.
23. W. P. Heal, B. Jovanovic, S. Bessin, M. H. Wright, A. I. Magee and E. W. Tate, *Chem. Commun.*, 2011, **47**, 4081-4083.
24. X. Zhou and G. Arthur, *J. Lipid Res.*, 1992, **33**, 1233-1236.
25. G. Loving and B. Imperiali, *J. Am. Chem. Soc.*, 2008, **130**, 13630-13638.
26. J. Folch, M. Lees and G. H. Sloane Stanley, *J. Biol. Chem.*, 1957, **226**, 497-509.
27. Y. Xu, J. F. Heilier, G. Madalinski, E. Genin, E. Ezan, J. C. Tabet and C. Junot, *Anal. Chem.*, 2010, **82**, 5490-5501.
28. M. Haque, Y. Hirai, K. Yokota, N. Mori, I. Jahan, H. Ito, H. Hotta, I. Yano, Y. Kanemasa and K. Oguma, *J. Bacteriol.*, 1996, **178**, 2065-2070.
29. J. R. Vestal and D. C. White, *Bioscience*, 1989, **39**, 535-541.
30. H. Q. Nguyen, R. A. Davis and J. Gervay-Hague, *Angew. Chem., Int. Ed.*, 2014, **53**, 13400-13403.
31. H. Kuge, K. Akahori, K. Yagyu and K. Honke, *J. Biol. Chem.*, 2014, **289**, 26783-26793.
32. M. K. Mishra, T. Kumaraguru, G. Sheelu and N. W. Fadnavis, *Tetrahedron-Asymmetry*, 2009, **20**, 2854-2860.
33. J. Lessig, J. Schiller, J. Arnhold and B. Fuchs, *J. Lipid Res.*, 2007, **48**, 1316-1324.
34. R. A. Davis, C. H. Lin and J. Gervay-Hague, *Chem. Commun.*, 2012, **48**, 9083-9085.
35. H. Tsugawa, H. Suzuki, H. Saya, M. Hatakeyama, T. Hirayama, K. Hirata, O. Nagano, J. Matsuzaki and T. Hibi, *Cell Host Microbe*, 2012, **12**, 764-777.
36. N. Murata-Kamiya, K. Kikuchi, T. Hayashi, H. Higashi and M. Hatakeyama, *Cell Host Microbe*, 2010, **7**, 399-411.
37. S. M. Campbell, S. M. Crowe and J. Mak, *J. Clin. Virol.*, 2001, **22**, 217-227.
38. J. S. Shin, Z. Gao and S. N. Abraham, *Science*, 2000, **289**, 785-788.
39. R. J. Schroeder, S. N. Ahmed, Y. Zhu, E. London and D. A. Brown, *J. Biol. Chem.*, 1998, **273**, 1150-1157.
40. J. Benting, A. Rietveld, I. Ansorge and K. Simons, *FEBS Lett.*, 1999, **462**, 47-50.
41. S. Arni, S. A. Keilbaugh, A. G. Ostermeyer and D. A. Brown, *The J. Biol. Chem.*, 1998, **273**, 28478-28485.
42. K. A. Melkonian, A. G. Ostermeyer, J. Z. Chen, M. G. Roth and D. A. Brown, *J. Biol. Chem.*, 1999, **274**, 3910-3917.
43. W. Rodgers, B. Crise and J. K. Rose, *Mol. Cell Biol.*, 1994, **14**, 5384-5391.
44. R. Brewster and S. A. Safran, *Biophys. J.*, 2010, **98**, L21-23.
45. S. Grille, A. Zaslawski, S. Thiele, J. Plat and D. Warnecke, *Prog. Lipid Res.*, 2010, **49**, 262-288.